Acoustic Imaging-Based UAV Sound Source Separation Technology.

Lingzhi Wang[1], Tianlun He[2], Da Chen[3,*]

[1]College of Transportation Science and Engineering, Civil Aviation University of China, Tianjin 300300, China
[2]School of Precision Instrument and Opto-electronics Engineering, Tianjin university, Tianjin 300072, China
[3]Center for Aviation Energy Environment and Green Development Research and Engineering, Tianjin 300300, China

Abstract. To address the key technical challenge of accurately separating and localizing noise sources from the propellers of quadrotor UAVs, this paper innovatively proposes an acoustic imaging method based on a 64-channel multi-arm logarithmic spiral array combined with the CLEAN-SC beamforming algorithm. The influence of array configuration on sound source identification performance was systematically investigated, and the results demonstrate that the multi-arm logarithmic spiral array with a diameter of 0.8 meters provides significant advantages in both dynamic range and angular resolution. Compared to traditional methods, this study achieves high-precision separation and imaging of the four propeller sound sources by leveraging the synergistic effect of an optimized array configuration and an advanced beamforming algorithm. Both simulations and experimental measurements in hovering scenarios validate the effectiveness of the proposed method, offering important insights for UAV noise control and structural optimization design.

1 Introduction

In recent years, unmanned aerial vehicles (UAVs) have found widespread application across numerous fields such as logistics, aerial photography, agriculture, inspection,and firefighting. As a solution for the "last mile" of logistics, they have demonstrated immense potential and value[1,2]. However, since UAVs are predominantly deployed in airspace above densely populated communities, the noise they generate is perceived as more annoying and discomforting on a psychoacoustic level compared to traditional transportation sources such as road vehicles and aircraft[3,4].

To gain a deeper understanding of UAV noise characteristics and advance acoustic performance optimization,acoustic imaging technology has gradually emerged as a research hotspot. He Jingyu et al.[5] have achieved localization and imaging of overall UAV noise, but refinement in separating key noise sources—particularly the propellers—remains insufficient.

Achieving component-level sound source separation and imaging requires targeted imaging methods. Traditional beamforming techniques[6,7], while robust and fastin imaging, are limited by issues such as low resolution and side lobe interference. To address these limitations, Sijtsma[8] proposed the CLEAN-SC deconvolution algorithm, which significantly improves resolution by suppressing side lobes.

Extensive research has been conducted on UAV noise by many scholars[9]. Although progress has been made, fine-grained separation and imaging of key noise sources—particularly the propellers—remain inadequate, and traditional beamforming methods are still constrained by low resolution and side lobe interference. To address these challenges, this study designs a 64-channel, 0.8-meter-aperture multi-arm logarithmic spiral array and employs the CLEAN-SC algorithm, ultimately achieving high-precision separation and imaging of multi-rotor UAVpropeller noise sources. This work provides an importanttechnical foundation for UAV propeller noise control.

2 Acoustic Imaging Algorithms

2.1. Conventional Beamforming

In acoustic imaging algorithms, Conventional Beamforming enables rapid imaging. The estimated acoustic source power A at each grid point obtained by conventional beamforming:

$$A\left(\xi_j\right)=\frac{1}{2}\frac{\boldsymbol{g}_j^*\left\langle \boldsymbol{p}\boldsymbol{p}^*\right\rangle \boldsymbol{g}_j}{\left\|\boldsymbol{g}_j\right\|^4}=\boldsymbol{w}_j^*\boldsymbol{C}\boldsymbol{w}_j \tag{1}$$

In them, $\boldsymbol{g}_j$ is the steering vector , $\boldsymbol{g}_j^*$ represents the complex conjugate transpose of $\boldsymbol{g}_j$, and $\boldsymbol{w}_j$ is the weighted steering vector.

2.2 CLEAN-SC Algorithm

CLEAN-SC (CLEAN based on spatial source coherence)beamforming algorithm can remove sidelobes

* Corresponding author: chenda@cauc.edu.cn

that interfere with acoustic source imaging, thereby enhancing the angular resolution of the array. The principle and methodology are defined by the following equation.

$$\boldsymbol{p}_k \boldsymbol{p}_k^* = \frac{\left(A\left(\xi_j\right)\right)^2 \boldsymbol{h}_j \boldsymbol{h}_j^*}{\left|\boldsymbol{p}_k^* \boldsymbol{w}_j\right|^2} \approx A\left(\xi_j\right) \boldsymbol{h}_j \boldsymbol{h}_j^* \tag{2}$$

In them, $\boldsymbol{h}_j$ represents the source component, and $\boldsymbol{p}_k$ is the source vector.

3 Array Performance Simulation and Optimization

3.1. Different Array Configurations

The subject of this study is a quadcopter unmanned aerial vehicle (UAV). During flight, its noise is primarily generated by the rotation of the four propellers, with the noise frequency mainly concentrated below 3 kHz[10]. The frequency of the acoustic source signals set and processed in this paper is 3000 Hz. This choice is based on consideration of the Rayleigh limit[11]. There is a positive correlation between the signal frequency and the angular resolution of the array. If the frequency is too low, the angular resolution will significantly decrease, making it difficult to distinguish between adjacent sound sources.

Different array configurations affect the dynamic range of the array, which in turn influences resolution performance. In line with the spectral characteristics of the UAV, experiments were conducted to compare and analyze the performance of various array configurations while maintaining the same number of microphones, as shown in Figure 1. Among them, all four array types consist of 32 microphones. The multi-arm spoke array and the multi-arm logarithmic spiral array have a minimum radius of 0.05 m and a maximum radius of 0.2 m.

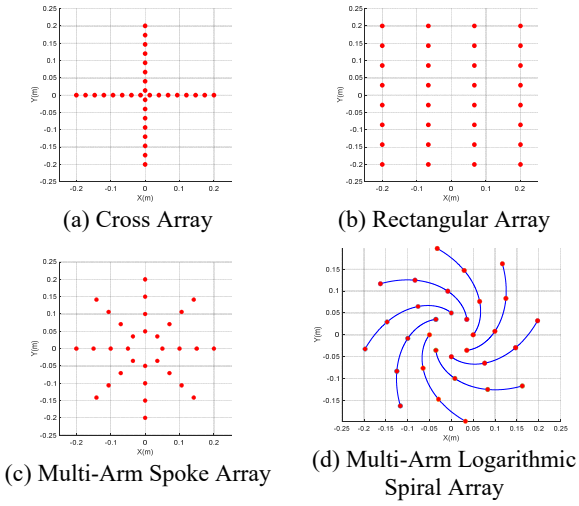

(a) Cross Array (b) Rectangular Array

(c) Multi-Arm Spoke Array (d) Multi-Arm Logarithmic Spiral Array

Figure 1. Common Microphone Array Configurations

In array performance analysis, dynamic range is a key metric for evaluating array capabilities—a larger dynamic range indicates stronger suppression of sidelobe interference. Figure 2 compares the variation of dynamic range with frequency for the four array configurations. At the operating frequency of 3 kHz, the multi-arm logarithmic spiral array exhibits a larger dynamic range than the other arrays, measuring 7.6 dB, thus demonstrating optimal performance.

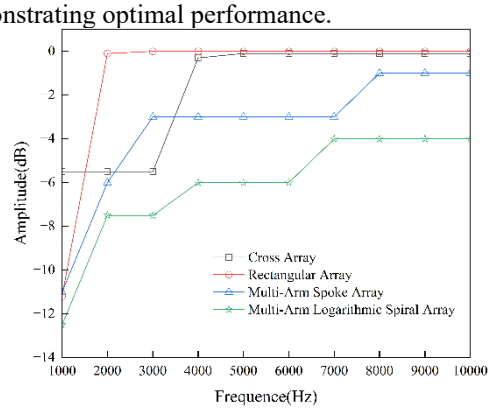

Figure 2. Dynamic Range Distribution of Four Microphone Array Configurations

3.2. Array Optimization

The number of microphones and the array aperture are critical factors influencing imaging performance. The array aperture determines the minimum resolvable angle of the system, while the number of microphones affects spatial sampling. Therefore, to enhance the resolution of the array, the number of array elements and the aperture sizeare increased on this basis. A total of six multi-arm logarithmic spiral arrays with varying numbers of elements and aperture sizes, as shown in Figure 3, were generated. Figure 4 illustrates the dynamic range variations of these six array configurations.

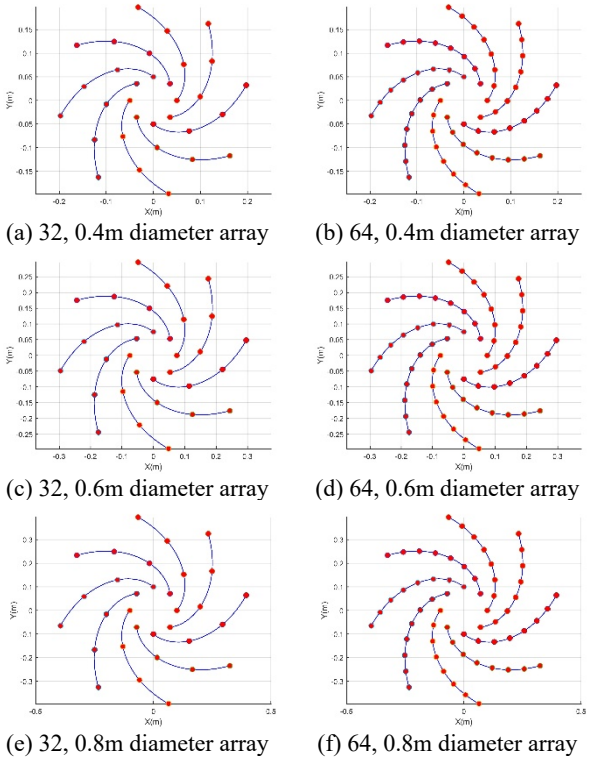

(a) 32, 0.4m diameter array (b) 64, 0.4m diameter array

(c) 32, 0.6m diameter array (d) 64, 0.6m diameter array

(e) 32, 0.8m diameter array (f) 64, 0.8m diameter array

Figure 3. Six-Arm Log-Spiral Arrays with Varying Element Count and Aperture Size

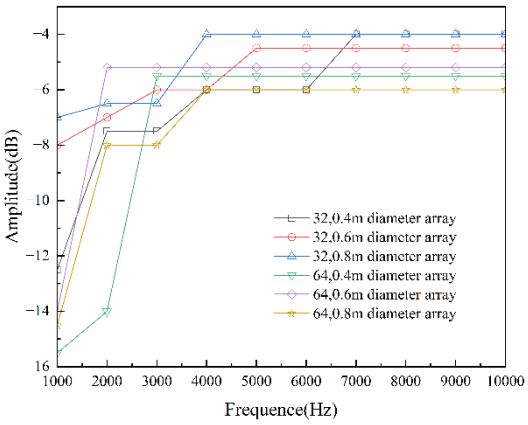

Figure 4. Dynamic Range Distributions of Six Microphone Array Configurations

To evaluate the acoustic imaging performance of different arrays, we compared six distinct array configurations. The experimental results clearly demonstrate that, as shown in Figure 4, the 64-channel, 0.8-meter aperture multi-arm logarithmic spiral array exhibits the most outstanding dynamic range performance. Compared to the other five tested array configurations, this spiral array structure can more effectively suppress sidelobe interference during acoustic source imaging, thereby significantly enhancing the clarity and accuracy of sound source localization.

4 Research on Sound Source Separation and Imaging

Based on the insightful findings obtained from the aforementioned simulation results, a dedicated experimental setup was meticulously constructed to validate the performance in a real-world scenario. As illustrated in Figure 5, the experimental configuration featured two cross-fixed plates, which were precisely positioned 1 meter in front of the center of the microphone array. These plates were specifically designed to simulate the structural frame of a UAV and to provide secure mounts for the fixed motors. The four motors were arranged to form a perfect rectangle, with dimensions measuring exactly 32 cm by 32 cm, thereby replicating a typical UAV propulsion layout.

For acoustic data acquisition, a multi-arm logarithmic spiral array, composed of 64 high-sensitivity microphones and boasting an aperture of 0.8 meters, was employed. This particular array was selected due to its superior performance identified in the earlier comparative analysis. During the experiment, the rotational speed of the propellers was consistently maintained at 5000 revolutions per minute. The microphone array was then utilized to collect the acoustic data generated by the rotating propellers, with the data acquisition parameters set to a sampling frequency of 32 kHz and a sampling interval of 0.1 seconds to ensure high-fidelity signal capture.

The acoustic source imaging results, processed using the conventional beamforming algorithm at a source frequency of 3000 Hz, are presented in Figure 6. Upon examination of the figure, it is evident that the acoustic signals emanating from the four individual propellers are successfully localized. They are clearly resolved and presented as four distinct and separable sound sources against the imaging plane.

Furthermore, Figure 7 showcases the acoustic source map derived from applying the CLEAN-SC beamforming algorithm to the same dataset. In stark contrast to the results obtained with conventional beamforming, the CLEAN-SC algorithm demonstrates a marked and significant improvement in angular resolution. The sources appear considerably sharper and more concentrated, effectively suppressing sidelobe interference and providing a much clearer and more precise representation of the source locations.

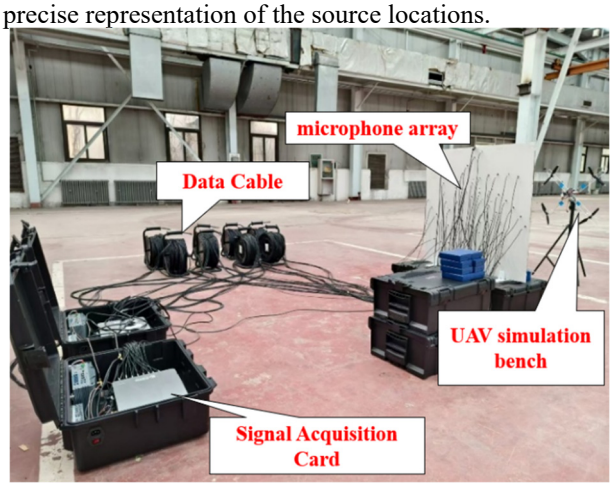

Figure 5. Equipment Composition and Setup of the Experimental Scene

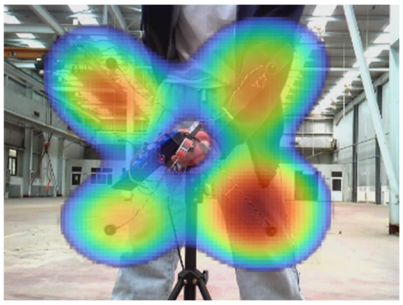

Figure 6. Conventional Beamforming Imaging Results

Figure 7. CLEAN-SC Algorithm Imaging Results

The aforementioned simulation experiments have validated the effectiveness of the multi-arm logarithmic spiral array combined with the CLEAN-SC algorithm in static scenarios. However, during actual flight, UAVs are influenced by factors such as motion states,

environmental noise, and airflow disturbances, which may significantly alter their acoustic source characteristics. To verify the practical applicability of the method, further real-world flight experiments were conducted.

The experiment employed a custom-built heavy-duty drone with dimensions of 0.33 m × 0.33 m. During the experiment, it was hovered at an altitude of 1 m above the array to collect audio data. Figures 8 and 9 show the imaging results of conventional beamforming and the CLEAN-SC algorithm, respectively, at a frequency of 3 kHz.

The experimental results indicate that the conventional beamforming algorithm struggles to effectively separate the acoustic source signals from the four propellers of the drone. This is mainly due to two reasons: first, interference from airflow during flight and fuselage vibration noise; second, the limited resolution of the conventional beamforming algorithm, which causes the acoustic sources from the four propellers to become aliased in the image and prevents their separation.

This deficiency is mitigated by the CLEAN-SC beamforming algorithm, as illustrated in Figure 9. The CLEAN-SC algorithm significantly enhances the angular resolution, suppresses a substantial amount of sidelobe interference, and distinctly reveals four separated acoustic sources.

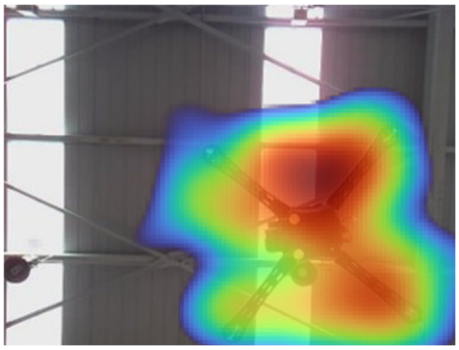

Figure 8. Conventional Beamforming Imaging Results

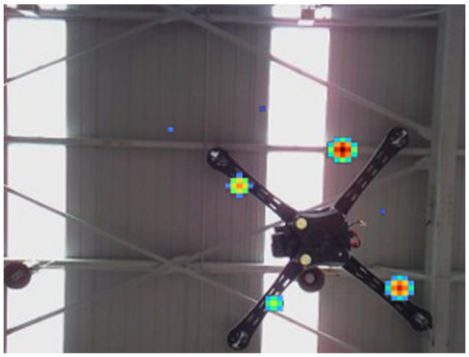

Figure 9. CLEAN-SC Algorithm Imaging Results

5 Summary

This study effectively addresses the technical challenge of acoustic source separation and imaging for the propellers of a quadcopter drone by employing an optimized multi-arm logarithmic spiral array and the CLEAN-SC beamforming algorithm. The results demonstrate that the 64-channel, 0.8m aperture multi-arm logarithmic spiral array exhibits excellent acoustic performance, while the CLEAN-SC algorithm successfully overcomes the limitations of conventional beamforming methods in terms of resolution and sidelobe suppression. Experiments confirm that this system can achieve precise separation and spatial localization of drone propeller noise, providing an effective technical approach for noise characteristic research and noise reduction design.

References

1. Li X C, Liu Z X. Application of UAV delivery in the "last mile" of rural logistics [J]. Logistics Technology, 2024, 47(19): 62-65.
2. Ying J F. Application of UAV surveying and mapping in comprehensive management projects of water conservancy and flood control [J]. Waterborne Safety, 2024, (22): 4-6.
3. Christian A W, Cabell R. Initial investigation into the psychoacoustic properties of small unma-nned aerial system noise[C]//23rd AIAA/CEAS aeroacoustics conference. 2017: 4051.
4. Gwak D Y, Han D, Lee S. Sound quality factors influencing annoyance from hovering UAV[J]. Journal of sound and vibration, 2020, 489: 115651.
5. He J Y, Liu J Z, Yang Z C, et al. Development and testing of a noise source tracking and localization systemfor multi-rotor UAVs [J]. Modern Defence Technology, 2024, 52(3): 1-8.
6. Van Veen B D, Buckley K M. Beamforming: A versatile approach to spatial filtering[J]. IEEE assp magazine, 1988, 5(2): 4-24.
7. Pillai S U. Array signal processing[M]. Springer Science & Business Media, 2012.
8. Sijtsma P. CLEAN based on spatial source coherence[J]. International journal of aeroacoustics, 2007, 6(4): 357-374.
9. Ramos-Romero C, Green N, Torija A J, et al. On-field noise measurements and acoustic characterisation of multi-rotor small unmanned aerial systems[J]. Aerospace Science and Technology, 2023, 141: 108537.
10. Cao S. Design and implementation of an acoustic array detection system for small UAVs [D]. Chongqing University of Technology, 2024.
11. Aldeman M, Raman G. Effects of array scaling and advanced beamforming algorithms on the angular resolution of microphone array systems[J]. Applied Acoustics, 2018, 132: 58-81.